iScience

CellPress
OPEN ACCESS

Article

Oral vancomycin treatment suppresses gut trypsin activity and preserves intestinal barrier function during EAE

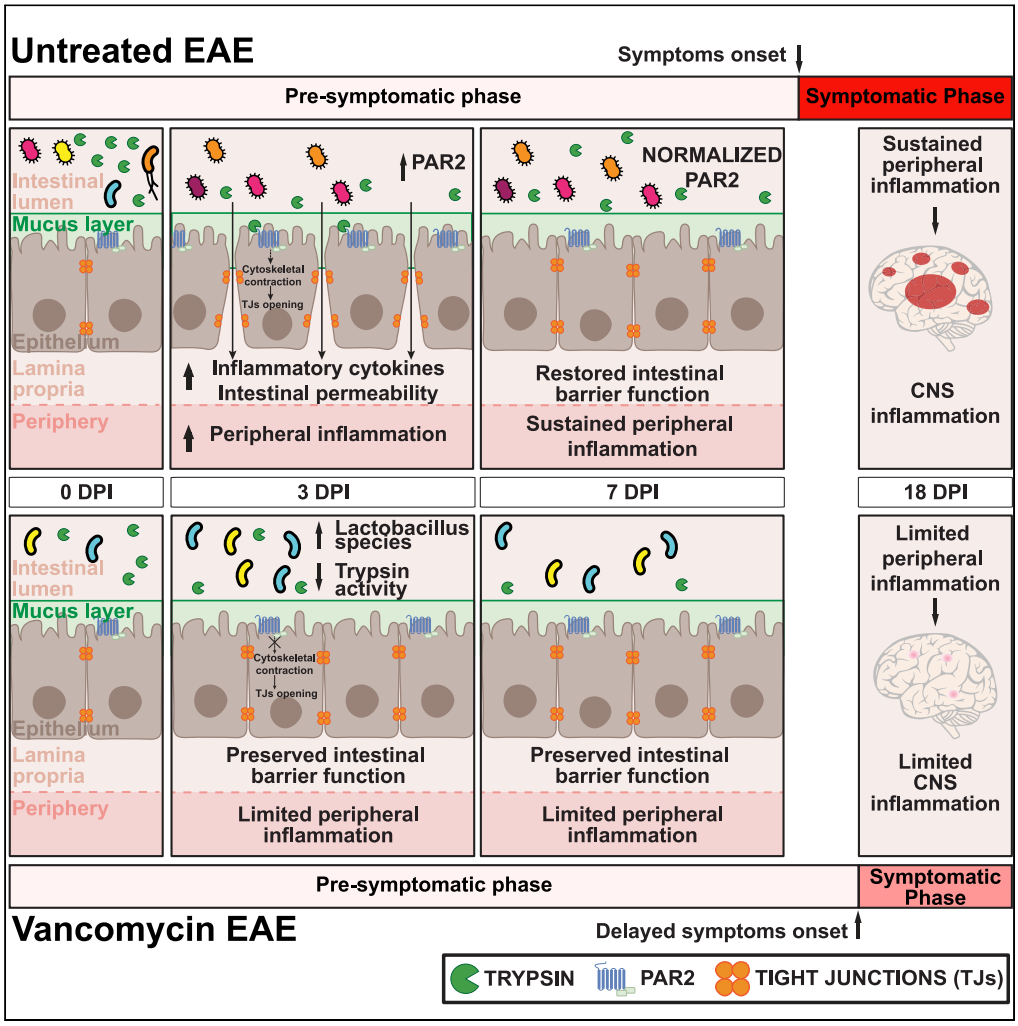

Paola Bianchimano, Kacper Iwanowski, Emma M. Smith, ..., Howard L. Weiner, Jose C. Clemente, Stephanie K. Tankou

stephanie.tankou@mssm.edu

Highlights

Increased intestinal epithelium PAR2 expression and gut permeability during EAE

Decreased trypsin activity and intact gut permeability in EAE mice on vancomycin

Gut trypsin activity is modulated by the gut microbiota

Gut trypsin activity and EAE severity negatively correlate with *Lactobacillus* taxa

Bianchimano et al., iScience 26, 108143
November 17, 2023
https://doi.org/10.1016/j.isci.2023.108143

iScience

CellPress
OPEN ACCESS

Article

Oral vancomycin treatment suppresses gut trypsin activity and preserves intestinal barrier function during EAE

Paola Bianchimano,[1,2,3,10] Kacper Iwanowski,[1,2,3,10] Emma M. Smith,[1,2,3] Adam Cantor,[3,4] Paola Leone,[1,2,3] Gerold Bongers,[3] Carlos G. Gonzalez,[5] Yoon Hongsup,[6,7,11] Joshua Elias,[8] Howard L. Weiner,[9] Jose C. Clemente,[3,4] and Stephanie K. Tankou[1,2,3,12,*]

SUMMARY

Studies have reported increased intestinal permeability in multiple sclerosis (MS) patients and its mouse model experimental autoimmune encephalomyelitis (EAE). However, the mechanisms driving increased intestinal permeability that in turn exacerbate neuroinflammation during EAE remain unclear. Here we showed that vancomycin preserved the integrity of the intestinal barrier, while also suppressing gut trypsin activity, enhancing the relative abundance of specific *Lactobacilli* and ameliorating disease during EAE. Furthermore, *Lactobacilli* enriched in the gut of vancomycin-treated EAE mice at day 3 post immunization negatively correlated with gut trypsin activity and EAE severity. In untreated EAE mice, we observed increased intestinal permeability and increased intestinal protease activated receptor 2 (PAR2) expression at day 3 post immunization. Prior studies have shown that trypsin increases intestinal permeability by activating PAR2. Our results suggest that the interaction between intestinal PAR2 and trypsin may be a key modulator of intestinal permeability and disease severity during EAE.

INTRODUCTION

Multiple sclerosis (MS) is a chronic central nervous system (CNS) inflammatory and neurodegenerative disease characterized by demyelination and neuroaxonal loss.[1–3] MS is thought to be initiated by autoreactive lymphocytes that cross the blood-brain barrier and mount an inflammatory reaction against the CNS myelin proteins.[4]

The gut-brain axis refers to the bidirectional pathways linking brain and gut functions. The gut microbiota and the intestinal barrier, key players in the gut-brain axis, have been the focus of a lot of attention due to their emerging role in mediating health and disease and potential use as therapeutic targets. The gut-brain axis disruption may participate in the pathophysiology of several brain disorders, including MS.[5–10] Several studies have reported altered gut microbiota composition and impaired intestinal barrier in MS and its animal model, experimental autoimmune encephalomyelitis (EAE).[11–18] The intestinal barrier has several functions including absorbing nutrients and metabolites as well as maintaining intestinal microbes, toxins, and other antigens in the gut lumen.[19] The key components of the intestinal barrier are the intestinal immune system, the epithelial layer which regulates paracellular permeability or "gut leakiness", secretory products such as antimicrobial peptides, the mucus lining which creates physical separation between the epithelium and luminal contents, and immunoglobulin A (IgA) which is carried along the mucus lining.[13,20] The intestinal epithelium consists of a single layer of highly specialized cells held together by more than 50 transmembrane tight junction (TJ) proteins.[20,21] TJ proteins form a physical barrier between the apical and basolateral epithelial compartments and selectively regulate passive diffusion of ions and water-soluble molecules through the paracellular pathway.[22,23] The three major TJ proteins are occludin, claudins, and junctional adhesion molecule proteins.[24] TJ proteins expression is regulated by several factors including microbial-derived metabolites.[25–28]

[1]Department of Neurology, Icahn School of Medicine at Mount Sinai, New York, NY, USA
[2]Friedman Brain Institute, Icahn School of Medicine at Mount Sinai, New York, NY, USA
[3]Precision Immunology Institute, Icahn School of Medicine at Mount Sinai, New York, NY, USA
[4]Department of Genetics and Genomic Sciences, Icahn School of Medicine at Mount Sinai, New York, NY, USA
[5]Department of Pharmacology, University of California San Diego, San Diego, CA 92093, USA
[6]Institute of Clinical Neuroimmunology, Hospital and Biomedical Center of the Ludwig-Maximilian-University, Martinsried, Germany
[7]Hertie Senior Professor Group, Max-Plank-Institute of Neurobiology, Martinsried, Germany
[8]Mass Spectrometry Platform, Chan Zuckerberg Biohub, San Francisco, CA 94158, USA
[9]Ann Romney Center for Neurologic Diseases, Harvard Medical School, Brigham and Women's Hospital, Boston, MA, USA
[10]These authors contributed equally
[11]Present address: School of Life Science, Handong Global University, Pohang, Gyungbuk, Republic of Korea
[12]Lead contact
*Correspondence: stephanie.tankou@mssm.edu
https://doi.org/10.1016/j.isci.2023.108143

Increased intestinal permeability or "leaky gut" can cause unregulated passage of luminal contents into the host[12,29] and subsequent activation of immune cells by otherwise non-immunogenic commensal microbes. A leaky gut is a common hallmark of inflammatory diseases.[12,29–33] Prior studies reported that relapsing-remitting MS (RRMS) patients are more likely to have compromised intestinal permeability.[16,17]

As in MS patients, EAE mice develop increased intestinal barrier permeability.[11,14] These intestinal alterations were observed after adoptive transfer of myelin oligodendrocyte glycoprotein-reactive (MOG-reactive) $CD4^+$ T cells, suggesting that circulating autoreactive T cells are critical to induce gut alterations. However, the mechanisms accounting for increased intestinal permeability in EAE mice or MS patients are poorly understood. Prior reports implicating zonulin aka haptoglobin 2 precursor (HP2) as a master regulator of TJ proteins expression, promoting TJ disassembly,[34] need to be revisited as studies have demonstrated that the commercial zonulin ELISA is neither adequate to measure intestinal permeability nor the postulated biomarker zonulin.[35] Furthermore, a study reporting increased zonulin in the gut of EAE mice is misleading since zonulin is not naturally expressed in mice.[11]

We previously reported that vancomycin-treated mice are protected from EAE.[36] We have also observed that vancomycin treatment reduces gut proteases level.[37] Interestingly, aberrant protease activity contributes to the loss of intestinal barrier integrity and to chronic inflammation.[38] Gut proteases can increase intestinal permeability by either directly degrading intestinal TJs or acting as signaling molecules via proteolytic activation of protease activated receptors (PARs).[39] Four receptors have been identified in the PARs family,[40] and activation of these G protein-coupled receptors occurs after the proteolytic cleavage of the N-terminal extracellular tail, releasing a new N terminus that functions as a tethered ligand. In the gut, PARs are expressed on epithelial cells, endothelial cells, neurons, inflammatory cells, mast cells, smooth muscle cells, and fibroblasts. Most of the research on intestinal permeability involves PAR2. Studies have shown that PAR2 activation by the serine proteases trypsin, tryptase, and chymase increases intestinal permeability.[41–43] Increased intestinal permeability following PAR2 activation is mediated through the activation of myosin light-chain kinase, resulting in myosin light chain hyperphosphorylation and opening of the intestinal TJs.[39]

We previously reported that in mice with mild EAE, serine protease inhibitor levels reached a peak at 3 days post immunization (DPI) whereas serine protease inhibitor levels in mice with severe EAE did not change during the pre-symptomatic stage of the disease.[37] Given that protease inhibitors block proteases activity, these findings led us to hypothesize that gut proteases activity at 3 DPI may be an important modulator of disease severity in EAE mice. So far, no studies have investigated the role of gut proteases in EAE mice or MS patients. In the current study, we investigated whether and how the interplay between vancomycin and the gut microbiota alters intestinal permeability, gut trypsin activity, and disease severity during EAE. We reported that vancomycin treatment suppressed gut trypsin activity, preserved intestinal permeability, and ameliorated disease during EAE at least in part by promoting an increase in the abundance of specific *Lactobacillus* species at 3 DPI. In untreated EAE mice, we observed increased intestinal permeability and increased intestinal PAR2 expression at 3 DPI whereas gut trypsin activity was unchanged. Our results suggest that intestinal PAR2-trypsin interaction at 3 DPI might be an important modulator of gut permeability and EAE severity.

RESULTS

Preserved intestinal permeability and decreased gut trypsin activity in vancomycin-treated EAE mice

We previously reported that vancomycin ameliorates EAE and that this protective effect is mediated via the gut microbiota.[36] Given prior reports that intestinal permeability is increased in EAE mice and that the gut microbiota modulates gut permeability,[14] we investigated the effect of vancomycin on intestinal permeability during the pre-symptomatic phase of EAE. We focused on the pre-symptomatic phase of EAE because we previously observed a negative correlation between EAE severity and serine protease inhibitor levels at 3 DPI.[37] Given that protease inhibitors' primary function is to block proteases activity and since proteases are important regulators of gut permeability, our findings led us to hypothesize that increased gut proteases activity at 3 DPI could be the main driver of increased intestinal permeability during the pre-symptomatic phase of EAE. Hence, 8-week-old C57BL/6J mice were gavaged with sodium fluorescein (NaF), and 3 h later, blood was collected at 0, 3, and 7 DPI with myelin oligodendrocyte glycoprotein amino acids 35–55 (MOG_{35-55}) in untreated and vancomycin-treated mice (Figures 1A and 1B). To evaluate the relative contribution of a CNS antigen-specific response versus the sole contribution of the complete Freund adjuvant (CFA), another group of mice was immunized with CFA only. In agreement with prior studies, we found increased intestinal permeability in untreated EAE mice at 3 DPI as assessed *in vivo* by the luminal to blood passage of the fluorescent marker, sodium fluorescein (Figure 1C). Only mice immunized with antigen MOG_{35-55} displayed increased gut permeability. However, we observed no change in intestinal permeability in vancomycin-treated EAE mice (Figure 1D). Furthermore, untreated EAE mice displayed increased intestinal permeability compared to vancomycin-treated mice during the pre-symptomatic phase of EAE (Figure 1E). Given that a previous study reported downregulation of mRNA coding for intestinal TJ proteins in EAE mice,[14] we next examined the expression of zonula occludens-1, -2, and -3 (ZO-1, ZO-2, ZO-3), occludin, and claudin-2 and -8 in the gut of untreated and vancomycin-treated mice. We observed no significant changes in the expression of these TJ proteins between pre- and post-EAE induction states in untreated EAE mice as measured by quantitative real-time PCR (Figure S1). Hence, our results indicated that EAE induction did not alter the expression of these TJ proteins, and as such, the increase in intestinal permeability seen in our untreated EAE mice cannot be explained by decreased gene expression of ZO-1 and claudin-8 as previously reported.[14] We found that vancomycin-treated EAE mice had increased ZO-1 expression compared to untreated EAE mice (Figure S1). Hence, one possible mechanism by which vancomycin treatment preserved intestinal barrier function is via promoting the upregulation of ZO-1.

We have previously reported decreased gut serine protease levels in vancomycin-treated mice.[37] Given that gut trypsin (a serine protease) has been shown to modulate intestinal permeability, we next measured the level of gut trypsin in untreated and vancomycin-treated mice. We

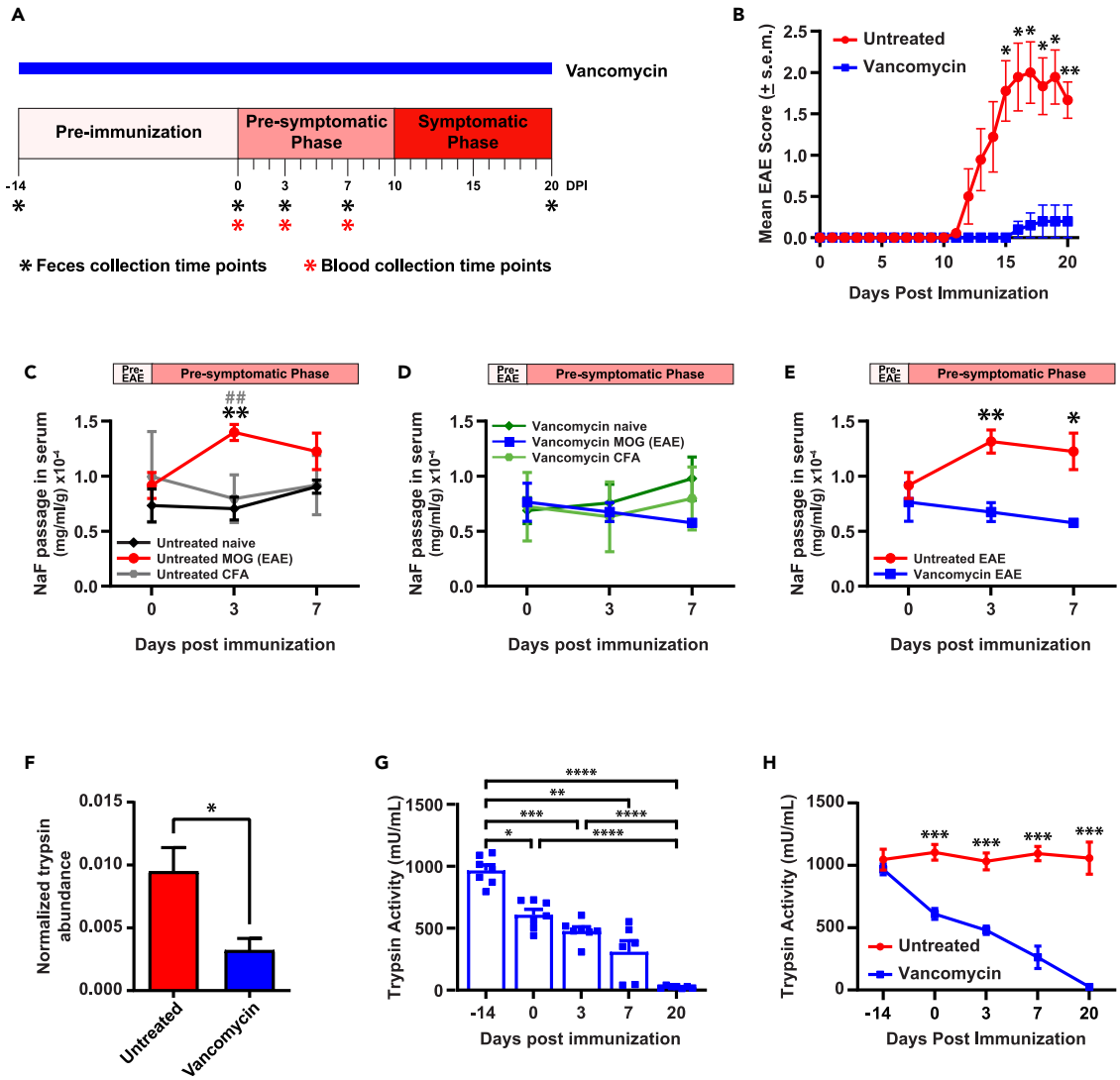

Figure 1. Preserved intestinal permeability and decreased gut trypsin activity in vancomycin-treated EAE mice

(A) Schematic design. Mice received either water (untreated; n = 8) or vancomycin (n = 8), and 2 weeks later, they were immunized with PBS and CFA or MOG_{35-55} and CFA (EAE mice). Blood samples and feces were collected at the indicated time points.

(B) EAE mean clinical scores in Untreated EAE (Untreated) and Vancomycin-treated EAE (Vancomycin) mice (mean ± SEM); representative data of three independent experiments. Data were analyzed using a Mixed-effects model followed by Bonferroni's post-test for multiple comparisons.

(C–E) *In vivo* intestinal permeability was assessed using sodium fluorescein (NaF). Representative data of three independent experiments with n = 6–8 mice/group. Data were analyzed using a mixed-effects model followed by Tukey's or Sydák's correction for multiple comparisons (mean ± SEM). (C) Intestinal permeability in untreated naive mice, and untreated mice immunized with MOG and CFA (Untreated EAE) or PBS and CFA (Untreated CFA). **p < 0.01 (Difference between Untreated EAE and Untreated naive mice), ##p < 0.01 (Difference between Untreated EAE and Untreated CFA mice). (D) Intestinal permeability in vancomycin-treated naive mice (vancomycin naive), and vancomycin-treated mice immunized with PBS and CFA (Vancomycin CFA) or MOG and CFA (Vancomycin EAE). (E) Intestinal permeability in untreated and vancomycin-treated EAE mice during the pre-symptomatic phase of EAE.

(F) Stool trypsin abundance was assessed 3 days after EAE induction using mass spectrometry. Trypsin levels were analyzed using Kolmogorov-Smirnov non-parametric test (mean +SEM; n = 8).

(G and H) Fecal trypsin activity was measured at the indicated time points. Representative data of three independent experiments with n = 7–8 mice/group. Results were analyzed using a mixed-effects model followed by Tukey's or Bonferroni's post-test for multiple comparisons. (G) Trypsin activity in Vancomycin-treated EAE mice (mean +SEM). (H) Trypsin activity in Untreated and Vancomycin-treated EAE mice (mean ± SEM). See also Figure S2. *p < 0.05; **p < 0.01; ***p < 0.001; ****p < 0.0001.

found decreased gut trypsin level in vancomycin-treated mice compared to untreated mice at 3 DPI (Figure 1F).[37] We next examined gut trypsin activity in untreated and vancomycin-treated mice during EAE. We observed decreased mean gut trypsin activity in vancomycin-treated mice (Figures 1G and 1H). We did not observe any change in mean gut trypsin activity in untreated EAE mice (Figure S2).

Increased intestinal PAR2 expression during EAE

Activation of intestinal PAR2 by trypsin triggers signaling pathways that lead to opening of TJs and increased intestinal permeability. We observed increased gut permeability in untreated EAE mice at 3 DPI despite the fact that gut trypsin activity remained unchanged during EAE. Hence, we hypothesized that, at 3 DPI, increased intestinal PAR2 expression could be an important driver of increased intestinal permeability during EAE. To determine if increased intestinal permeability in untreated EAE mice was driven by change in PAR2 expression, we examined intestinal PAR2 expression in EAE mice. We found increased PAR2 expression in the ileum of untreated EAE mice at 3 DPI compared to naive and vancomycin-treated EAE mice (Figure 2A). At 7 DPI, intestinal PAR2 expression in untreated EAE mice was comparable to that observed in naive (Figure 2B). At 18 DPI (peak EAE), intestinal PAR2 expression in untreated EAE mice was increased compared to naive and vancomycin-treated EAE mice (Figure 2C). Given that PAR2 is also expressed on immune cells which could thus skew the PAR2 signal we observed, we isolated epithelial cells from the gut of naive mice as well as untreated EAE mice at disease peak and confirmed increased PAR2 expression on gut-derived epithelial cells from untreated EAE mice compared to naive mice by quantitative real-time PCR (Figure 2D). We further confirmed this finding by performing western blot to assess the expression of intestinal PAR2 at the protein level in EAE mice at disease peak. We found 1.5-fold increased PAR2 expression in the ileum of EAE mice compared to naive or CFA-only immunized mice (Figures 2E and 2F). Hence, these results suggest that increased intestinal PAR2 expression may be one mechanism accounting for increased gut permeability in untreated EAE mice.

Vancomycin treatment had no significant effect on intestinal PAR2 expression during EAE. Hence, these results suggest that PAR2 expression may not be primarily modulated by the gut microbiota.

The gut microbiota modulates gut trypsin activity

Given our findings that vancomycin suppressed trypsin activity, we next investigated if trypsin activity was modulated via the gut microbiota. Hence, we measured stool trypsin activity in untreated and vancomycin-treated conventionally raised mice as well as germ-free (GF) mice. We observed decreased gut trypsin activity in the stool of germ-free mice compared to untreated and vancomycin-treated conventionally raised mice (Figure 3A). These data showed that the gut microbiota modulates gut trypsin activity. Given that vancomycin-treated mice had decreased gut trypsin activity compared to untreated mice, we next collected feces at 5 time points spanning pre- and post-EAE induction (Figures 1A and 1B) to perform 16S rRNA profiling. As expected, vancomycin-treated EAE mice had decreased alpha diversity at all time points (Figure 3B). The untreated and vancomycin-treated EAE mice segregated into distinct communities at 3 DPI ($q = 0.004$; Figure 3C). As expected, we observed a change in the abundance of several bacteria between vancomycin-treated and untreated mice including *Lactobacillus species* during the pre-symptomatic phase of the disease (Figure 3D). We observed that four *Lactobacillus* species including *L. frumenti*, *L. reuteri*, *L. vaginalis*, and *Lactobacillus frumenti/reuteri/antri/oris/panis/vaginalis* (*L. f/r/a/o/p/v*) were enriched in vancomycin-treated mice, with their relative abundance peaking at 3 DPI (Figures 3E–3H). In untreated EAE mice, no change in the relative abundance of these four *Lactobacillus* species was observed (Figures 3E–3H). In untreated EAE mice, we observed decreased relative abundance of *Barnesiella intestinihominis* (Figure 3I) and increased relative abundance of *Turicibacter sanguinis* (Figure 3J) during the pre-symptomatic phase of EAE.

Lactobacillus species enriched in vancomycin-treated EAE mice negatively correlate with gut trypsin activity and EAE severity

To identify gut commensals that are associated with gut trypsin activity and EAE severity, we performed correlations under the influence (CUTIE)[44] correlation analysis on all the mice. We found that four *Lactobacillus* species including *L. reuteri*, *L. frumenti*, *L. vaginalis*, and *L. f/r/a/o/p/v* negatively correlated with trypsin activity and EAE severity during the pre-symptomatic phase of the disease (Figures 4A and 4C). Interestingly, these same four *Lactobacillus* species were enriched in the gut of vancomycin-treated EAE mice during the pre-symptomatic phase of the disease (Figures 3E–3H). Furthermore, prior studies have reported that *L. reuteri* and *L. frumenti* preserve the integrity of the intestinal barrier.[45–49] Taken together, these results suggested that one possible mechanism accounting for preserved intestinal permeability in vancomycin-treated EAE mice was increased relative abundance of *Lactobacillus* species that might suppress gut trypsin activity. Even though mean gut trypsin activity did not change overtime in the untreated EAE mice group, we did observe intragroup variability in gut trypsin activity (Figure S2). Hence, we also examined correlation between bacteria abundance and gut trypsin activity in the untreated EAE mice group only. We observed that *Barnesiella intestinihominis* negatively correlates with gut trypsin activity in untreated EAE mice (Figures 4B and 4D). Interestingly, one study reports that *B. intestinihominis* positively correlated with preserved intestinal permeability.[50] Furthermore, we found that *B. intestinihominis* abundance was decreased at 3 DPI in untreated EAE mice (Figure 3I). Hence, these results suggest that one possible mechanism that may contribute to increased gut permeability at 3 DPI in untreated EAE is decreased abundance of *B. intestinihominis* leading to increased gut trypsin activity. We also observed four bacterial species including *Turicibacter sanguinis* that positively correlated with gut trypsin activity during the pre-symptomatic phase of EAE (Figures 4B, 4D, and S3).

DISCUSSION

Increased intestinal permeability has been reported in MS and EAE mice and is believed to play a role in the pathophysiology of the disease.[11,14,16,17] Increased intestinal permeability also referred to as "leaky gut" leads to translocation of gut microbes and microbial-derived products into the periphery, and this subsequently leads to increased peripheral and CNS inflammation.[12,29] However, the mechanisms accounting for increased intestinal permeability in MS and EAE mice are poorly understood.

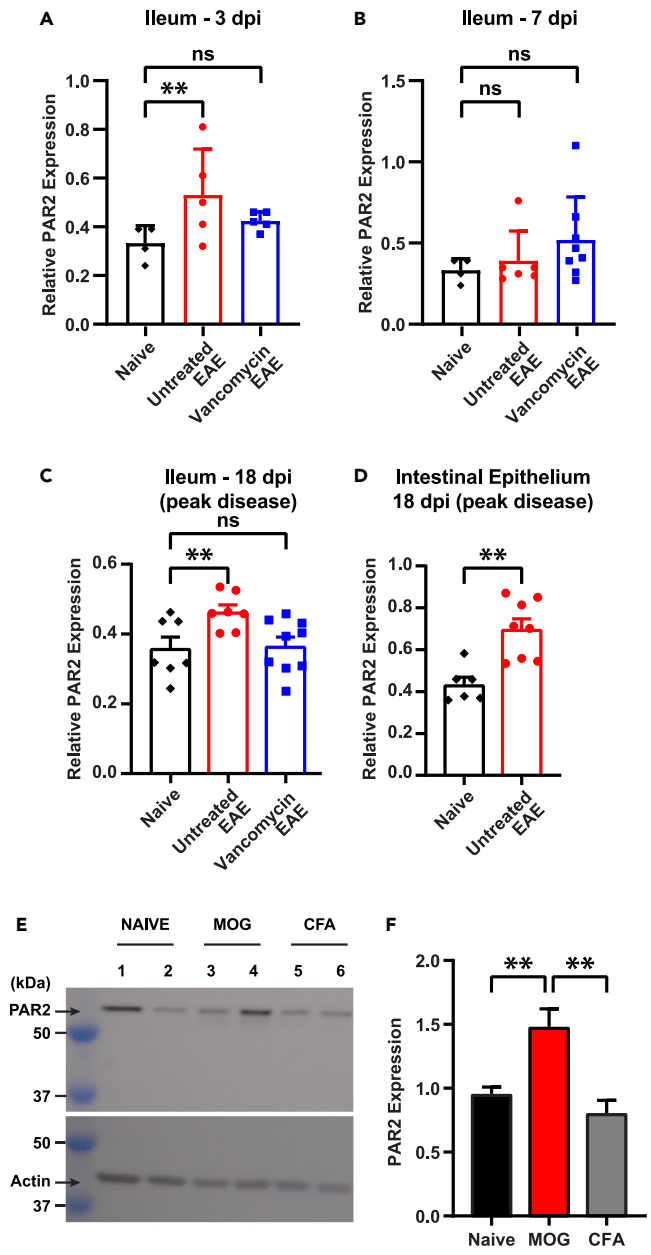

Figure 2. Increased intestinal PAR2 expression during EAE

Increased intestinal PAR2 expression during EAE (A–D). Protease Activated Receptor 2 (PAR2) expression was measured by quantitative PCR (qPCR) in the ileum (A–C) and intestinal epithelium (D) at the indicated time points. Representative data of two independent experiments. Results were analyzed using the Kruskal-Wallis non-parametric test followed by Dunn's multiple comparisons test. Multiple comparisons test was performed comparing the mean rank of PAR2 expression in untreated and vancomycin-treated EAE mice with the mean rank PAR2 expression in naive mice. Results are expressed as mean +SEM, with individual values (n = 4–8).

(E) PAR2 protein expression was assessed by western blot on ileum samples from naive mice as well as mice immunized with PBS and CFA (CFA) or PBS and MOG (MOG) during peak EAE.

(F) PAR2 expression in the ileum of naive, MOG-immunized, and CFA-immunized mice was normalized to β-actin. Representative data of three independent experiments. Data were analyzed using a one-way ANOVA followed by Tukey's multiple comparisons test (mean +SEM; n = 3–5). **p < 0.01; ns: not significant.

In this study, we found that untreated EAE mice displayed increased gut permeability at 3 DPI whereas vancomycin-treated EAE mice had preserved intestinal barrier function. We have previously reported increased intestinal serine protease inhibitor levels at 3 DPI in untreated EAE mice with mild disease compared to untreated EAE mice with severe disease.[37] Given that the main function of protease inhibitors is to suppress proteases activity and that proteases are important modulator of gut permeability, these findings led us to hypothesize that, during

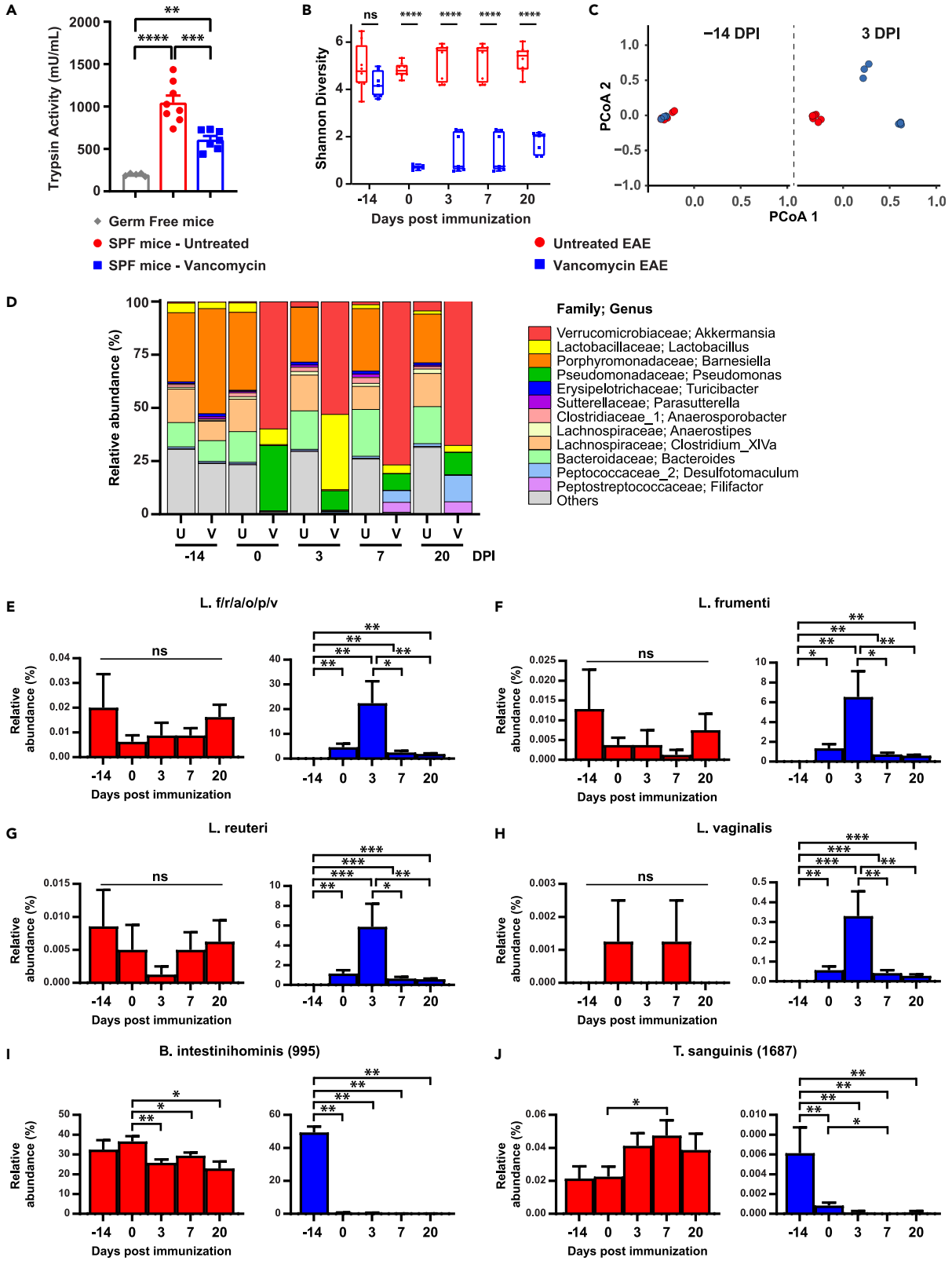
A
Trypsin Activity (mU/mL)
Germ Free mice
SPF mice - Untreated
SPF mice - Vancomycin
B
Shannon Diversity
Days post immunization
C
−14 DPI
3 DPI
PCoA 2
PCoA 1
Untreated EAE
Vancomycin EAE
D
Relative abundance (%)
DPI
Family; Genus
Verrucomicrobiaceae; Akkermansia
Lactobacillaceae; Lactobacillus
Porphyromonadaceae; Barnesiella
Pseudomonadaceae; Pseudomonas
Erysipelotrichaceae; Turicibacter
Sutterellaceae; Parasutterella
Clostridiaceae_1; Anaerosporobacter
Lachnospiraceae; Anaerostipes
Lachnospiraceae; Clostridium_XlVa
Bacteroidaceae; Bacteroides
Peptococcaceae_2; Desulfotomaculum
Peptostreptococcaceae; Filifactor
Others
E
L. f/r/a/o/p/v
F
L. frumenti
G
L. reuteri
H
L. vaginalis
I
B. intestinihominis (995)
J
T. sanguinis (1687)
Relative abundance (%)
Days post immunization

Figure 3. The gut microbiota modulates gut trypsin activity

(A) Fecal trypsin activity in germ-free mice, untreated, and vancomycin-treated naive specific pathogen-free (SPF) mice. Data were analyzed using one-way ANOVA followed by Tukey's multiple comparisons test (mean +SEM; n = 5–8).

(B) Shannon's α-diversity was calculated at a sampling depth of 5,000 reads per sample. Data were analyzed using a mixed-effects model followed by Sydák's correction for multiple comparisons. Results are presented as median with interquartile ranges, whiskers represent Min and Max values, individual values are shown (n = 7–8).

(C) Principal coordinate analysis of intestinal microbiota samples based on Bray Curtis shows significantly different clustering between untreated and vancomycin-treated EAE mice at 3 DPI (q = 0.004). Each dot represents the microbiota from one mouse.

(D) Taxa plots showing compositional differences in fecal microbiota at the indicated time points in untreated (U) and vancomycin-treated (V) EAE mice.

(E–J) Bar plots showing changes in the relative abundance of selected species during EAE in Untreated (red) and Vancomycin-treated mice (blue). *p < 0.05; **p < 0.01; ***p < 0.001; ****p < 0.0001; ns: not significant (p > 0.05). *L. f/r/a/o/p/v*: *Lactobacillus frumenti/reuteri/antri/oris/panis/vaginalis*.

EAE, gut proteases activity reaches its peak at 3 DPI and this translates into increased gut intestinal permeability which will subsequently lead to severe disease. We observed decreased gut trypsin activity in vancomycin-treated EAE mice whereas trypsin activity was unchanged in untreated EAE mice. Given prior reports that gut trypsin promotes the opening of intestinal TJs via activation of intestinal PAR2, we examined the expression of PAR2 during EAE. We found increased intestinal PAR2 expression in untreated EAE mice at 3 DPI whereas PAR2 expression did not significantly changed in vancomycin-treated EAE mice. Our findings suggest that the decreased intestinal permeability observed in vancomycin-treated EAE mice may at least in part be due to decreased gut trypsin activity leading to decreased signaling downstream intestinal PAR2 which keeps the intestinal TJs close thereby preserving intestinal barrier function and subsequently suppressing peripheral and CNS inflammation. In support of these findings, prior studies have shown that oral administration of Bowman-Birk or PETIR001 serine protease inhibitors attenuated neuroinflammation and neurodegeneration in EAE mice.[51–53] The protective effects of serine protease inhibitors in EAE mice were at least in part due to delayed infiltration of encephalitogenic cells into the CNS as well as increased interleukin-10 (IL-10) secretion.[54,55] Our results suggest that one possible mechanism accounting for delayed infiltration of inflammatory cells in the CNS of EAE mice following serine protease inhibitor treatment could be preserved gut barrier function due to decreased gut trypsin activity. Interestingly, several studies have reported altered serine protease levels in MS sera, cerebrospinal fluid, and CNS lesions.[56,57] Prior studies have reported that serine proteases play key regulatory roles in inflammatory processes through various mechanisms including direct modification of chemokine and cytokine activity, activation of receptors, cleavage of adhesion molecules, induction of CXCL2, CXCL8, CCL2, MCP-1, and IL-8 expression, activation of TLR4, and induction and activation of matrix metalloproteases in the periphery and/or CNS.[58,59] However to this date, no study has investigated the role of gut serine proteases in EAE and/or MS. This study is the first report on the role of gut trypsin on intestinal permeability in EAE mice.

Our findings suggest that in untreated EAE mice, increased intestinal PAR2 expression during the pre-symptomatic phase of EAE may lead to more trypsin-PAR2 interaction which leads to activation of more PAR2, intestinal TJs opening, and subsequent increased intestinal permeability eventually leading to increased peripheral and CNS inflammation. Hence, increased intestinal PAR2 expression at 3 DPI might be the *sine qua non* for triggering the cascade of events that will promote the transition from pre-symptomatic phase to symptomatic phase of EAE. These findings suggest that intestinal PAR2 antagonists could potentially ameliorate disease in MS and other immune-mediated diseases characterized by increased gut permeability. Interestingly, one study reports that total PAR2 knockout (KO) mice are protected from EAE.[60] Our findings suggest that a possible explanation for disease amelioration in these PAR2 KO mice is preserved intestinal barrier function. Hence, future studies should generate intestinal epithelial cells-specific PAR2 KO mice to determine if intestinal PAR2 modulates neuroinflammation during EAE. Prior studies have reported that inflammatory cytokines like tumor necrosis factor alpha (TNF-α) increases endothelial PAR2 expression.[61] Hence, we examined levels of various pro-inflammatory cytokines and chemokines in the ileum of naive as well as untreated and vancomycin-treated EAE mice to determine if changes in cytokines expression might be driving increased intestinal PAR2 during the pre-symptomatic phase of EAE and at disease peak (Figure S4). TNF-α was the only cytokine that was increased in untreated EAE mice compared to naive and vancomycin-treated mice at 3 DPI (Figure S4). During the pre-symptomatic phase of EAE, untreated and vancomycin-treated EAE mice had comparable levels of pro-inflammatory cytokines and chemokines (Figure S4). Hence, these findings suggest that pro-inflammatory cytokines may not be the main modulator of intestinal PAR2 expression during the pre-symptomatic phase of EAE.

Since trypsin is known to modulate the immune response, it is conceivable that gut trypsin could be contributing to inflammatory damage in EAE through several mechanisms. Gut trypsin might potentially also contribute to the pathogenesis of EAE by activating pro-inflammatory cytokines and chemokines as well as priming encephalitogenic cells infiltrating the small intestine and colon.

We demonstrated that the gut microbiota modulates gut trypsin activity. Interestingly, a recent study reported that certain gut bacteria can degrade trypsin.[62] We observed that vancomycin treatment promotes the enrichment of *L. frumenti* and *L. reuteri* which have been shown to preserve intestinal barrier function.[45–49] Furthermore, a prior study reported that *L. reuteri* ameliorates EAE.[63] During the pre-symptomatic phase of EAE, we found a negative correlation between the abundance of *L. reuteri*, *L. frumenti*, *L. vaginalis*, and *L. f/r/a/o/p/v* and gut trypsin activity as well as EAE severity. These findings suggest that vancomycin treatment induced increased abundance of *Lactobacillus* species that may suppress trypsin activity leading to decreased trypsin-intestinal PAR2 interaction which in turn leads to decreased PAR2 activation thereby keeping the TJs close and preserving intestinal barrier function. These results suggest that the abundance of *L. reuteri*, *L. frumenti*, *L. vaginalis*, and *L. f/r/a/o/p/v* during the pre-symptomatic phase of EAE could be a biomarker of disease severity. Future studies should investigate if these *Lactobacillus* species can also be used as biomarker of disease severity in patients with radiographically isolated syndrome (pre-symptomatic phase of MS).[1] The mechanism by which these *Lactobacillus* species suppress trypsin activity is unknown. Given

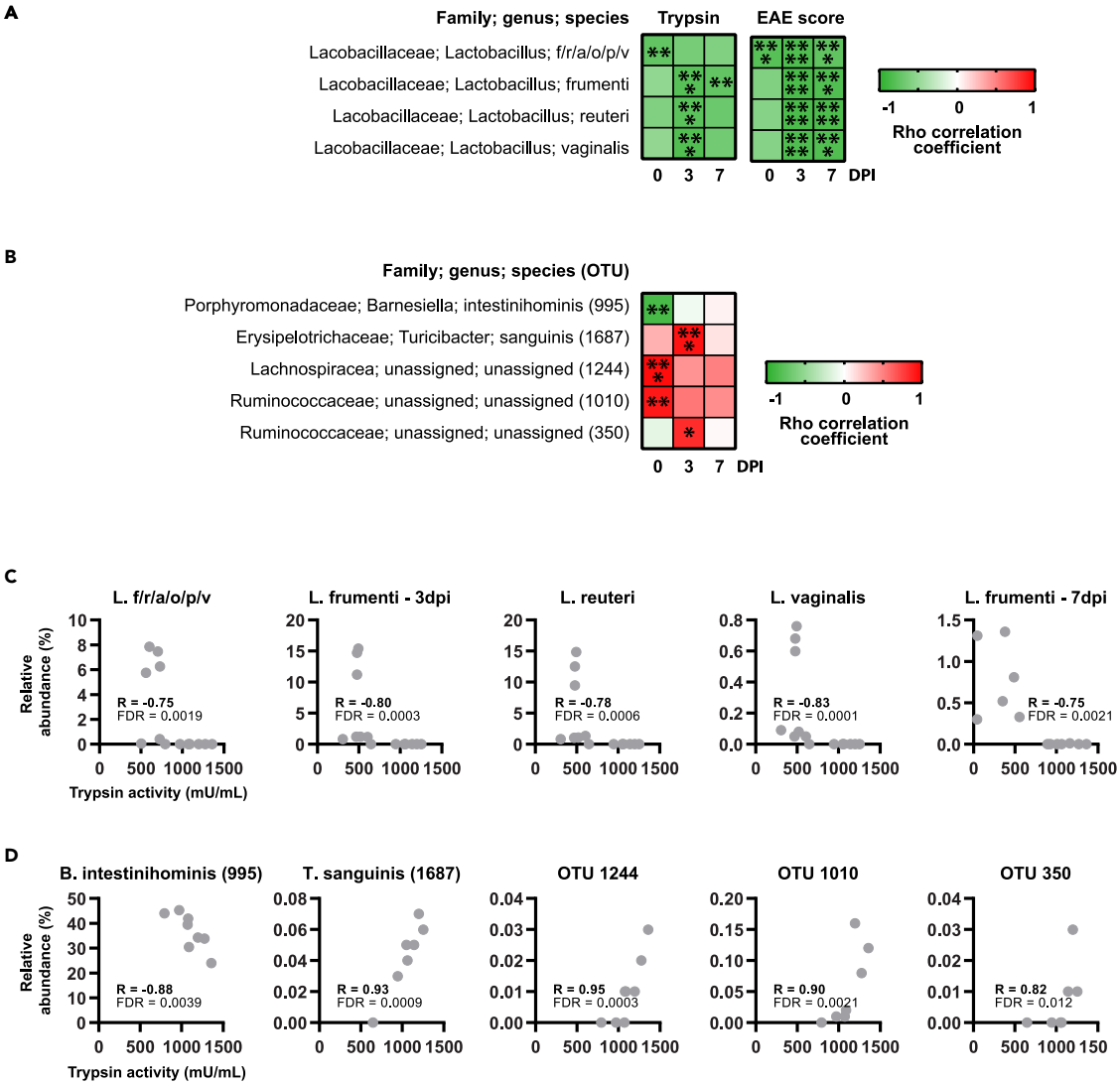

Figure 4. Lactobacilli negatively correlate with gut trypsin activity and EAE severity

Correlations between relative abundance of indicated taxa and fecal trypsin activity or cumulative EAE clinical score using CUTIE correlation analysis.

(A) Correlation matrix for selected taxa showing significant (FDR <0.05) correlations with trypsin activity and EAE score at the indicated time points. *p < 0.05; **p < 0.01; ***p < 0.001; ****p < 0.0001.

(B) Correlation matrix showing significant (FDR <0.05) correlations between selected taxa and trypsin activity in untreated EAE mice at the indicated time points. See also Figure S3.

(C) Scatterplots of selected taxa showing significant correlations with trypsin activity. *L. f/r/a/o/p/v*: *Lactobacillus frumenti/reuteri/antri/oris/panis/vaginalis*.OTU350: Ruminococcaceae; unassigned; OTU1010: Ruminococcacea, unassigned; OTU1244: Lachnospiraceae; unassigned.

prior report that certain gut bacteria belonging to *Paraprevotella* genus can degrade trypsin, future studies should investigate if these *Lactobacillus* species can also degrade trypsin via a different mechanism.

Taken together, our results suggest that one possible mechanism by which vancomycin preserves the integrity of the gut barrier is by suppressing trypsin activity which will eventually lead to attenuated disease. Furthermore, we have previously reported that another mechanism by which vancomycin ameliorates EAE is via promoting the proliferation of bacteria inducing regulatory T cells.[36] To assess if these protective effects of vancomycin are translatable to humans, we have launched a randomized, double-blind placebo-controlled trial to investigate the impact of vancomycin on the gut microbiome, peripheral immune function, and brain lesions load in MS patients (NCT05539729). This study could lead to the identification of gut-derived bacteria that are capable of inhibiting gut trypsin activity as well as attenuating peripheral and CNS inflammation in MS. These bacteria could then be developed into live biotherapeutic products for the prevention and treatment of MS.

Our results also suggest that oral PAR2 antagonists with poor bioavailability as well as serine protease inhibitors could be novel classes of drugs to prevent MS in high-risk individuals as well as those with radiographically isolated syndrome (pre-symptomatic phase of MS).

Limitations of the study

Here we report that vancomycin-treated mice have enriched *Lactobacilli* in their gut compared to untreated mice and this may lead to decreased gut trypsin activity, decreased signaling downstream of PAR2, and subsequently preservation of intestinal barrier function. We showed that there is a negative correlation between *Lactobacilli* abundance and gut trypsin activity in vancomycin-treated EAE mice. However, correlation does not imply causation. Hence, future studies should examine the effect of these *Lactobacilli* species on gut trypsin activity and investigate if these taxa can degrade trypsin.

STAR★METHODS

Detailed methods are provided in the online version of this paper and include the following:

- KEY RESOURCES TABLE
- RESOURCE AVAILABILITY
  - Lead contact
  - Materials availability
  - Data and code availability
- EXPERIMENTAL MODEL AND STUDY PARTICIPANT DETAILS
  - Animals
  - EAE induction
  - Vancomycin treatment
- METHOD DETAILS
  - Feces collection, processing, and storage
  - Tissue collection
  - Blood collection
  - In-vivo permeability assay
  - Trypsin activity assay
  - Quantitative real-time PCR
  - Immunoblotting
  - 16S rRNA gene sequencing and analysis
- QUANTIFICATION AND STATISTICAL ANALYSIS

SUPPLEMENTAL INFORMATION

Supplemental information can be found online at https://doi.org/10.1016/j.isci.2023.108143.

ACKNOWLEDGMENTS

This work was supported by the Department of Neurology, Icahn School of Medicine at Mount Sinai, NIH grant R01NS087226 from the National Institute of Neurological Disorders and Stroke (NINDS), and the National MS Society.

AUTHOR CONTRIBUTIONS

S.K.T., P.B., P.L., K.I., E.M.S., C.G.G., and G.B. performed experiments; P.B, A.C., and J.C.C. analyzed the microbiome data; C.G.G. and J.E. performed stool proteomics experiments; Y.H. assisted with animal experimentation; S.K.T., P.B., and G.B. generated the figures; S.K.T., P.B., and K.I. wrote the manuscript with input from all authors. S.K.T. conceived the study, designed the analysis, and finalized the manuscript. S.K.T. supervised the project.

DECLARATION OF INTERESTS

The authors declare no competing interests.

INCLUSION AND DIVERSITY

We support inclusive, diverse, and equitable conduct of research.

Received: April 18, 2023
Revised: August 30, 2023
Accepted: October 2, 2023
Published: October 6, 2023

SUPPORTING CITATIONS

The following references appear in the supplemental information: 73–79.

REFERENCES

1. Baecher-Allan, C., Kaskow, B.J., and Weiner, H.L. (2018). Multiple Sclerosis: Mechanisms and Immunotherapy. Neuron *97*, 742–768. https://doi.org/10.1016/j.neuron.2018.01.021.
2. Pérez, C.A., Cuascut, F.X., and Hutton, G.J. (2023). Immunopathogenesis, Diagnosis, and Treatment of Multiple Sclerosis A Clinical Update. Neurol. Clin. *41*, 87–106. https://doi.org/10.1016/j.ncl.2022.05.004.
3. Charabati, M., Wheeler, M.A., Weiner, H.L., and Quintana, F.J. (2023). Multiple sclerosis: Neuroimmune crosstalk and therapeutic targeting. Cell *186*, 1309–1327. https://doi.org/10.1016/j.cell.2023.03.008.
4. Murúa, S.R., Farez, M.F., and Quintana, F.J. (2021). The Immune Response in Multiple Sclerosis. Annu. Rev. Pathol. *17*, 1–19. https://doi.org/10.1146/annurev-pathol-052920-040318.
5. Carlson, A.L., Xia, K., Azcarate-Peril, M.A., Goldman, B.D., Ahn, M., Styner, M.A., Thompson, A.L., Geng, X., Gilmore, J.H., and Knickmeyer, R.C. (2018). Infant Gut Microbiome Associated With Cognitive Development. Biol. Psychiatr. *83*, 148–159. https://doi.org/10.1016/j.biopsych.2017.06.021.
6. Klingelhoefer, L., and Reichmann, H. (2015). Pathogenesis of Parkinson disease—the gut–brain axis and environmental factors. Nat. Rev. Neurol. *11*, 625–636. https://doi.org/10.1038/nrneurol.2015.197.
7. Kadowaki, A., and Quintana, F.J. (2020). The Gut–CNS Axis in Multiple Sclerosis. Trends Neurosci. *43*, 622–634. https://doi.org/10.1016/j.tins.2020.06.002.
8. Jiang, C., Li, G., Huang, P., Liu, Z., and Zhao, B. (2017). The Gut Microbiota and Alzheimer's Disease. J. Alzheimers Dis. *58*, 1–15. https://doi.org/10.3233/jad-161141.
9. Jangi, S., Gandhi, R., Cox, L.M., Li, N., von Glehn, F., Yan, R., Patel, B., Mazzola, M.A., Liu, S., Glanz, B.L., et al. (2016). Alterations of the human gut microbiome in multiple sclerosis. Nat. Commun. *7*, 12015. https://doi.org/10.1038/ncomms12015.
10. Cox, L.M., Maghzi, A.H., Liu, S., Tankou, S.K., Dhang, F.H., Willocq, V., Song, A., Wasén, C., Tauhid, S., Chu, R., et al. (2021). Gut Microbiome in Progressive Multiple Sclerosis. Ann. Neurol. *89*, 1195–1211. https://doi.org/10.1002/ana.26084.
11. Nouri, M., Bredberg, A., Weström, B., and Lavasani, S. (2014). Intestinal Barrier Dysfunction Develops at the Onset of Experimental Autoimmune Encephalomyelitis, and Can Be Induced by Adoptive Transfer of Auto-Reactive T Cells. PLoS One *9*, e106335. https://doi.org/10.1371/journal.pone.0106335.
12. Mirza, A., and Mao-Draayer, Y. (2017). The gut microbiome and microbial translocation in multiple sclerosis. Clin. Immunol. *183*, 213–224. https://doi.org/10.1016/j.clim.2017.03.001.
13. Buscarinu, M.C., Fornasiero, A., Romano, S., Ferraldeschi, M., Mechelli, R., Reniè, R., Morena, E., Romano, C., Pellicciari, G., Landi, A.C., et al. (2019). The Contribution of Gut Barrier Changes to Multiple Sclerosis Pathophysiology. Front. Immunol. *10*, 1916. https://doi.org/10.3389/fimmu.2019.01916.
14. Secher, T., Kassem, S., Benamar, M., Bernard, I., Boury, M., Barreau, F., Oswald, E., and Saoudi, A. (2017). Oral Administration of the Probiotic Strain Escherichia coli Nissle 1917 Reduces Susceptibility to Neuroinflammation and Repairs Experimental Autoimmune Encephalomyelitis-Induced Intestinal Barrier Dysfunction. Front. Immunol. *8*, 1096. https://doi.org/10.3389/fimmu.2017.01096.
15. Camara-Lemarroy, C.R., Silva, C., Greenfield, J., Liu, W.-Q., Metz, L.M., and Yong, V.W. (2020). Biomarkers of intestinal barrier function in multiple sclerosis are associated with disease activity. Mult. Scler. *26*, 1340–1350. https://doi.org/10.1177/1352458519863133.
16. Buscarinu, M.C., Cerasoli, B., Annibali, V., Policano, C., Lionetto, L., Capi, M., Mechelli, R., Romano, S., Fornasiero, A., Mattei, G., et al. (2017). Altered intestinal permeability in patients with relapsing–remitting multiple sclerosis: A pilot study. Mult. Scler. *23*, 442–446. https://doi.org/10.1177/1352458516652498.
17. Pellizoni, F.P., Leite, A.Z., Rodrigues, N.d.C., Ubaiz, M.J., Gonzaga, M.I., Takaoka, N.N.C., Mariano, V.S., Omori, W.P., Pinheiro, D.G., Matheucci Junior, E., et al. (2021). Detection of Dysbiosis and Increased Intestinal Permeability in Brazilian Patients with Relapsing–Remitting Multiple Sclerosis. Int. J. Environ. Res. Public Health *18*, 4621. https://doi.org/10.3390/ijerph18094621.
18. Camara-Lemarroy, C.R., Metz, L.M., and Yong, V.W. (2018). Focus on the gut-brain axis: Multiple sclerosis, the intestinal barrier and the microbiome. World J. Gastroenterol. *24*, 4217–4223. https://doi.org/10.3748/wjg.v24.i37.4217.
19. Chelakkot, C., Ghim, J., and Ryu, S.H. (2018). Mechanisms regulating intestinal barrier integrity and its pathological implications. Exp. Mol. Med. *50*, 1–9. https://doi.org/10.1038/s12276-018-0126-x.
20. Okumura, R., and Takeda, K. (2017). Roles of intestinal epithelial cells in the maintenance of gut homeostasis. Exp. Mol. Med. *49*, e338. https://doi.org/10.1038/emm.2017.20.
21. Lee, B., Moon, K.M., and Kim, C.Y. (2018). Tight Junction in the Intestinal Epithelium: Its Association with Diseases and Regulation by Phytochemicals. J. Immunol. Res. *2018*, 2645465. https://doi.org/10.1155/2018/2645465.
22. Odenwald, M.A., and Turner, J.R. (2013). Intestinal Permeability Defects: Is It Time to Treat? Clin. Gastroenterol. Hepatol. *11*, 1075–1083. https://doi.org/10.1016/j.cgh.2013.07.001.
23. Odenwald, M.A., and Turner, J.R. (2017). The intestinal epithelial barrier: a therapeutic target? Nat. Rev. Gastroenterol. Hepatol. *14*, 9–21. https://doi.org/10.1038/nrgastro.2016.169.
24. González-Mariscal, L., Betanzos, A., Nava, P., and Jaramillo, B.E. (2003). Tight junction proteins. Prog. Biophys. Mol. Biol. *81*, 1–44. https://doi.org/10.1016/s0079-6107(02)00037-8.
25. Slifer, Z.M., and Blikslager, A.T. (2020). The Integral Role of Tight Junction Proteins in the Repair of Injured Intestinal Epithelium. Int. J. Mol. Sci. *21*, 972. https://doi.org/10.3390/ijms21030972.
26. Tervonen, A., Ihalainen, T.O., Nymark, S., and Hyttinen, J. (2019). Structural dynamics of tight junctions modulate the properties of the epithelial barrier. PLoS One *14*, e0214876. https://doi.org/10.1371/journal.pone.0214876.
27. Ulluwishewa, D., Anderson, R.C., McNabb, W.C., Moughan, P.J., Wells, J.M., and Roy, N.C. (2011). Regulation of Tight Junction Permeability by Intestinal Bacteria and Dietary Components1,2. J. Nutr. *141*, 769–776. https://doi.org/10.3945/jn.110.135657.
28. Landy, J., Ronde, E., English, N., Clark, S.K., Hart, A.L., Knight, S.C., Ciclitira, P.J., and Al-Hassi, H.O. (2016). Tight junctions in inflammatory bowel diseases and inflammatory bowel disease associated colorectal cancer. World J. Gastroenterol. *22*, 3117–3126. https://doi.org/10.3748/wjg.v22.i11.3117.
29. Antonini, M., Lo Conte, M., Sorini, C., and Falcone, M. (2019). How the Interplay Between the Commensal Microbiota, Gut Barrier Integrity, and Mucosal Immunity Regulates Brain Autoimmunity. Front. Immunol. *10*, 1937. https://doi.org/10.3389/fimmu.2019.01937.
30. Vaarala, O. (2008). Leaking gut in type 1 diabetes. Curr. Opin. Gastroenterol. *24*, 701–706. https://doi.org/10.1097/mog.0b013e32830e6d98.
31. Audo, R., Sanchez, P., Rivière, B., Mielle, J., Tan, J., Lukas, C., Macia, L., Morel, J., and Immediato Daien, C. (2022). Rheumatoid arthritis is associated with increased gut permeability and bacterial translocation that are reversed by inflammation control. Rheumatology *62*, 1264–1271. https://doi.org/10.1093/rheumatology/keac454.
32. Antoni, L., Nuding, S., Wehkamp, J., and Stange, E.F. (2014). Intestinal barrier in inflammatory bowel disease. World J. Gastroenterol. *20*, 1165–1179. https://doi.org/10.3748/wjg.v20.i5.1165.
33. Fresko, I., Hamuryudan, V., Demir, M., Hızlı, N., Sayman, H., Melikoğlu, M., Tunç, R., Yurdakul, S., and Yazıcı, H. (2001). Intestinal permeability in Behçet's syndrome. Ann. Rheum. Dis. *60*, 65–66. https://doi.org/10.1136/ard.60.1.65.
34. Fasano, A. (2011). Zonulin and Its Regulation of Intestinal Barrier Function: The Biological Door to Inflammation, Autoimmunity, and Cancer. Physiol. Rev. *91*, 151–175. https://doi.org/10.1152/physrev.00003.2008.
35. Massier, L., Chakaroun, R., Kovacs, P., and Heiker, J.T. (2021). Blurring the picture in leaky gut research: how shortcomings of zonulin as a biomarker mislead the field of intestinal permeability. Gut *70*, 1801–1802. https://doi.org/10.1136/gutjnl-2020-323026.
36. Bianchimano, P., Britton, G.J., Wallach, D.S., Smith, E.M., Cox, L.M., Liu, S., Iwanowski, K., Weiner, H.L., Faith, J.J., Clemente, J.C., and Tankou, S.K. (2022). Mining the microbiota to identify gut commensals modulating

neuroinflammation in a mouse model of multiple sclerosis. Microbiome *10*, 174. https://doi.org/10.1186/s40168-022-01364-2.

37. Gonzalez, C.G., Tankou, S.K., Cox, L.M., Casavant, E.P., Weiner, H.L., and Elias, J.E. (2019). Latent-period stool proteomic assay of multiple sclerosis model indicates protective capacity of host-expressed protease inhibitors. Sci. Rep. *9*, 12460. https://doi.org/10.1038/s41598-019-48495-5.
38. Isozaki, Y., Yoshida, N., Kuroda, M., Handa, O., Takagi, T., Kokura, S., Ichikawa, H., Naito, Y., Okanoue, T., and Yoshikawa, T. (2006). Anti-tryptase treatment using nafamostat mesilate has a therapeutic effect on experimental colitis. Scand. J. Gastroenterol. *41*, 944–953. https://doi.org/10.1080/00365520500529470.
39. Van Spaendonk, H., Ceuleers, H., Witters, L., Patteet, E., Joossens, J., Augustyns, K., Lambeir, A.-M., De Meester, I., De Man, J.G., and De Winter, B.Y. (2017). Regulation of intestinal permeability: The role of proteases. World J. Gastroenterol. *23*, 2106–2123. https://doi.org/10.3748/wjg.v23.i12.2106.
40. Vergnolle, N. (2016). Protease inhibition as new therapeutic strategy for GI diseases. Gut *65*, 1215–1224. https://doi.org/10.1136/gutjnl-2015-309147.
41. Bjarnason, I., Macpherson, A., and Hollander, D. (1995). Intestinal permeability: An overview. Gastroenterology *108*, 1566–1581. https://doi.org/10.1016/0016-5085(95)90708-4.
42. Groschwitz, K.R., Wu, D., Osterfeld, H., Ahrens, R., and Hogan, S.P. (2013). Chymase-mediated intestinal epithelial permeability is regulated by a protease-activating receptor/matrix metalloproteinase-2-dependent mechanism. Am. J. Physiol. Gastrointest. Liver Physiol. *304*, G479–G489. https://doi.org/10.1152/ajpgi.00186.2012.
43. Róka, R., Demaude, J., Cenac, N., Ferrier, L., Salvador-cartier, C., Garcia-villar, R., Fioramonti, J., and Bueno, L. (2007). Colonic luminal proteases activate colonocyte proteinase-activated receptor-2 and regulate paracellular permeability in mice. Neuro Gastroenterol. Motil. *19*, 57–65. https://doi.org/10.1111/j.1365-2982.2006.00851.x.
44. Bu, K., Wallach, D.S., Wilson, Z., Shen, N., Segal, L.N., Bagiella, E., and Clemente, J.C. (2022). Identifying correlations driven by influential observations in large datasets. Briefings Bioinf. *23*, bbab482. https://doi.org/10.1093/bib/bbab482.
45. Schepper, J.D., Collins, F.L., Rios-Arce, N.D., Raehtz, S., Schaefer, L., Gardinier, J.D., Britton, R.A., Parameswaran, N., and McCabe, L.R. (2019). Probiotic Lactobacillus reuteri Prevents Postantibiotic Bone Loss by Reducing Intestinal Dysbiosis and Preventing Barrier Disruption. J. Bone Miner. Res. *34*, 681–698. https://doi.org/10.1002/jbmr.3635.
46. Hu, J., Chen, L., Zheng, W., Shi, M., Liu, L., Xie, C., Wang, X., Niu, Y., Hou, Q., Xu, X., et al. (2018). Lactobacillus frumenti Facilitates Intestinal Epithelial Barrier Function Maintenance in Early-Weaned Piglets. Front. Microbiol. *9*, 897. https://doi.org/10.3389/fmicb.2018.00897.
47. Nie, Y., Hu, J., Hou, Q., Zheng, W., Zhang, X., Yang, T., Ma, L., and Yan, X. (2019). Lactobacillus frumenti improves antioxidant capacity via nitric oxide synthase 1 in intestinal epithelial cells. Faseb. J. *33*, 10705–10716. https://doi.org/10.1096/fj.201900253rr.
48. Cui, Y., Liu, L., Dou, X., Wang, C., Zhang, W., Gao, K., Liu, J., and Wang, H. (2017). Lactobacillus reuteri ZJ617 maintains intestinal integrity via regulating tight junction, autophagy and apoptosis in mice challenged with lipopolysaccharide. Oncotarget *8*, 77489–77499. https://doi.org/10.18632/oncotarget.20536.
49. Lee, H.L., Kim, J.M., Moon, J.H., Kim, M.J., Jeong, H.R., Go, M.J., Kim, H.-J., Eo, H.J., Lee, U., and Heo, H.J. (2022). Anti-Amnesic Effect of Synbiotic Supplementation Containing Corni fructus and Limosilactobacillus reuteri in DSS-Induced Colitis Mice. Int. J. Mol. Sci. *24*, 90. https://doi.org/10.3390/ijms24010090.
50. Yao, H., Shi, Y., Yuan, J., Sa, R., Chen, W., and Wan, X. (2021). Matrine protects against DSS-induced murine colitis by improving gut barrier integrity, inhibiting the PPAR-α signaling pathway, and modulating gut microbiota. Int. Immunopharm. *100*, 108091. https://doi.org/10.1016/j.intimp.2021.108091.
51. Touil, T., Ciric, B., Ventura, E., Shindler, K.S., Gran, B., and Rostami, A. (2008). Bowman–Birk inhibitor suppresses autoimmune inflammation and neuronal loss in a mouse model of multiple sclerosis. J. Neurol. Sci. *271*, 191–202. https://doi.org/10.1016/j.jns.2008.04.030.
52. Gran, B., Tabibzadeh, N., Martin, A., Ventura, E.S., Ware, J.H., Zhang, G.-X., Parr, J.L., Kennedy, A.R., and Rostami, A.M. (2006). The protease inhibitor, Bowman-Birk Inhibitor, suppresses experimental autoimmune encephalomyelitis: a potential oral therapy for multiple sclerosis. Mult. Scler. *12*, 688–697. https://doi.org/10.1177/1352458506070769.
53. Reinhold, D., Bank, U., Entz, D., Goihl, A., Stoye, D., Wrenger, S., Brocke, S., Thielitz, A., Stefin, S., Nordhoff, K., et al. (2011). PETIR-001, a dual inhibitor of dipeptidyl peptidase IV (DP IV) and aminopeptidase N (APN), ameliorates experimental autoimmune encephalomyelitis in SJL/J mice. Biol. Chem. *392*, 233–237. https://doi.org/10.1515/bc.2011.024.
54. Dai, H., Ciric, B., Zhang, G.-X., and Rostami, A. (2011). Bowman–Birk inhibitor attenuates experimental autoimmune encephalomyelitis by delaying infiltration of inflammatory cells into the CNS. Immunol. Res. *51*, 145–152. https://doi.org/10.1007/s12026-011-8254-6.
55. Dai, H., Ciric, B., Zhang, G.-X., and Rostami, A. (2012). Interleukin-10 plays a crucial role in suppression of experimental autoimmune encephalomyelitis by Bowman–Birk inhibitor. J. Neuroimmunol. *245*, 1–7. https://doi.org/10.1016/j.jneuroim.2012.01.005.
56. Hjæresen, S., Sejbaek, T., Axelsson, M., Vinsløv-Jensen, H., Mortensen, S.K., Pihl-Jensen, G., Novakova, L., Christensen, J.D.R., Pedersen, C.B., Halle, B., et al. (2021). The levels of the serine protease HTRA1 in cerebrospinal fluid correlate with progression and disability in multiple sclerosis. J. Neurol. *268*, 3316–3324. https://doi.org/10.1007/s00415-021-10489-7.
57. Scarisbrick, I.A. (2008). Advances in multiple Sclerosis and Experimental Demyelinating Diseases. Curr. Top. Microbiol. Immunol. *318*, 133–175. https://doi.org/10.1007/978-3-540-73677-6_6.
58. Geraghty, P., Rogan, M.P., Greene, C.M., Boxio, R.M.M., Poiriert, T., O'Mahony, M., Belaaouaj, A., O'Neill, S.J., Taggart, C.C., and McElvaney, N.G. (2007). Neutrophil Elastase Up-Regulates Cathepsin B and Matrix Metalloprotease-2 Expression. J. Immunol. *178*, 5871–5878. https://doi.org/10.4049/jimmunol.178.9.5871.
59. Pham, C.T.N. (2006). Neutrophil serine proteases: specific regulators of inflammation. Nat. Rev. Immunol. *6*, 541–550. https://doi.org/10.1038/nri1841.
60. Noorbakhsh, F., Tsutsui, S., Vergnolle, N., Boven, L.A., Shariat, N., Vodjgani, M., Warren, K.G., Andrade-Gordon, P., Hollenberg, M.D., and Power, C. (2006). Proteinase-activated receptor 2 modulates neuroinflammation in experimental autoimmune encephalomyelitis and multiple sclerosis. J. Exp. Med. *203*, 425–435. https://doi.org/10.1084/jem.20052148.
61. Ritchie, E., Saka, M., MacKenzie, C., Drummond, R., Wheeler-Jones, C., Kanke, T., and Plevin, R. (2007). Cytokine upregulation of proteinase-activated-receptors 2 and 4 expression mediated by p38 MAP kinase and inhibitory kappa B kinase β in human endothelial cells. Br. J. Pharmacol. *150*, 1044–1054. https://doi.org/10.1038/sj.bjp.0707150.
62. Li, Y., Watanabe, E., Kawashima, Y., Plichta, D.R., Wang, Z., Ujike, M., Ang, Q.Y., Wu, R., Furuichi, M., Takeshita, K., et al. (2022). Identification of trypsin-degrading commensals in the large intestine. Nature *609*, 582–589. https://doi.org/10.1038/s41586-022-05181-3.
63. He, B., Hoang, T.K., Tian, X., Taylor, C.M., Blanchard, E., Luo, M., Bhattacharjee, M.B., Freeborn, J., Park, S., Couturier, J., et al. (2019). Lactobacillus reuteri Reduces the Severity of Experimental Autoimmune Encephalomyelitis in Mice by Modulating Gut Microbiota. Front. Immunol. *10*, 385. https://doi.org/10.3389/fimmu.2019.00385.
64. Kozich, J.J., Westcott, S.L., Baxter, N.T., Highlander, S.K., and Schloss, P.D. (2013). Development of a Dual-Index Sequencing Strategy and Curation Pipeline for Analyzing Amplicon Sequence Data on the MiSeq Illumina Sequencing Platform. Appl. Environ. Microbiol. *79*, 5112–5120. https://doi.org/10.1128/aem.01043-13.
65. Shaikh, F.Y., White, J.R., Gills, J.J., Hakozaki, T., Richard, C., Routy, B., Okuma, Y., Usyk, M., Pandey, A., Weber, J.S., et al. (2021). A Uniform Computational Approach Improved on Existing Pipelines to Reveal Microbiome Biomarkers of Nonresponse to Immune Checkpoint InhibitorsSingle Pipeline Reanalysis. Clin. Cancer Res. *27*, 2571–2583. https://doi.org/10.1158/1078-0432.ccr-20-4834.
66. Daquigan, N., Seekatz, A.M., Greathouse, K.L., Young, V.B., and White, J.R. (2017). High-resolution profiling of the gut microbiome reveals the extent of Clostridium difficile burden. NPJ Biofilms Microbiomes *3*, 35. https://doi.org/10.1038/s41522-017-0043-0.
67. Bolger, A.M., Lohse, M., and Usadel, B. (2014). Trimmomatic: a flexible trimmer for Illumina sequence data. Bioinformatics *30*, 2114–2120. https://doi.org/10.1093/bioinformatics/btu170.
68. Magoč, T., and Salzberg, S.L. (2011). FLASH: fast length adjustment of short reads to improve genome assemblies. Bioinformatics *27*, 2957–2963. https://doi.org/10.1093/bioinformatics/btr507.
69. Kuczynski, J., Stombaugh, J., Walters, W.A., González, A., Caporaso, J.G., and Knight, R. (2012). Using QIIME to Analyze 16S rRNA Gene Sequences from Microbial Communities. Curr. Protoc. Microbiol. *27*.

https://doi.org/10.1002/9780471729259.mc01e05s27.

70. Langmead, B., and Salzberg, S.L. (2012). Fast gapped-read alignment with Bowtie 2. Nat. Methods *9*, 357–359. https://doi.org/10.1038/nmeth.1923.
71. Wang, Q., Garrity, G.M., Tiedje, J.M., and Cole, J.R. (2007). Naïve Bayesian Classifier for Rapid Assignment of rRNA Sequences into the New Bacterial Taxonomy. Appl. Environ. Microbiol. *73*, 5261–5267. https://doi.org/10.1128/aem.00062-07.
72. Schneider, C.A., Rasband, W.S., and Eliceiri, K.W. (2012). NIH Image to ImageJ: 25 years of image analysis. Nat. Methods *9*, 671–675. https://doi.org/10.1038/nmeth.2089.
73. Kawane, K., Tanaka, H., Kitahara, Y., Shimaoka, S., and Nagata, S. (2010). Cytokine-dependent but acquired immunity-independent arthritis caused by DNA escaped from degradation. Proc. Natl. Acad. Sci. USA *107*, 19432–19437. https://doi.org/10.1073/pnas.1010603107.
74. Su, S.B., Grajewski, R.S., Luger, D., Agarwal, R.K., Silver, P.B., Tang, J., Tuo, J., Chan, C.-C., and Caspi, R.R. (2007). Altered Chemokine Profile Associated with Exacerbated Autoimmune Pathology under Conditions of Genetic Interferon-γ Deficiency. Invest. Ophthalmol. Vis. Sci. *48*, 4616–4625. https://doi.org/10.1167/iovs.07-0233.
75. Terashima, A., Watarai, H., Inoue, S., Sekine, E., Nakagawa, R., Hase, K., Iwamura, C., Nakajima, H., Nakayama, T., and Taniguchi, M. (2008). A novel subset of mouse NKT cells bearing the IL-17 receptor B responds to IL-25 and contributes to airway hyperreactivity. J. Exp. Med. *205*, 2727–2733. https://doi.org/10.1084/jem.20080698.
76. Duc, D., Vigne, S., Bernier-Latmani, J., Yersin, Y., Ruiz, F., Gaïa, N., Leo, S., Lazarevic, V., Schrenzel, J., Petrova, T.V., and Pot, C. (2019). Disrupting Myelin-Specific Th17 Cell Gut Homing Confers Protection in an Adoptive Transfer Experimental Autoimmune Encephalomyelitis. Cell Rep. *29*, 378–390.e4. https://doi.org/10.1016/j.celrep.2019.09.002.
77. Lin, J., Zhou, Z., Huo, R., Xiao, L., Ouyang, G., Wang, L., Sun, Y., Shen, B., Li, D., and Li, N. (2012). Cyr61 Induces IL-6 Production by Fibroblast-like Synoviocytes Promoting Th17 Differentiation in Rheumatoid Arthritis. J. Immunol. *188*, 5776–5784. https://doi.org/10.4049/jimmunol.1103201.
78. Tsai, P.-Y., Zhang, B., He, W.-Q., Zha, J.-M., Odenwald, M.A., Singh, G., Tamura, A., Shen, L., Sailer, A., Yeruva, S., et al. (2017). IL-22 Upregulates Epithelial Claudin-2 to Drive Diarrhea and Enteric Pathogen Clearance. Cell Host Microbe *21*, 671–681.e4. https://doi.org/10.1016/j.chom.2017.05.009.
79. Stephens, A.S., Stephens, S.R., and Morrison, N.A. (2011). Internal control genes for quantitative RT-PCR expression analysis in mouse osteoblasts, osteoclasts and macrophages. BMC Res. Notes *4*, 410. https://doi.org/10.1186/1756-0500-4-410.

STAR★METHODS

KEY RESOURCES TABLE

REAGENT or RESOURCE	SOURCE	IDENTIFIER
Antibodies		
Mouse Anti-Human-PAR-2 Antibody (SAM11) – HRP conjugated	Santa Cruz Biotechnology, Inc.	Cat#: SC-13504 HRP; RRID: AB_628101
Mouse Anti-Human Beta-Actin – HRP conjugated	Abcam	Cat# ab20272; RRID: AB_445482
Chemicals, peptides, and recombinant proteins		
MOG_{33-35} peptide	Genemed Synthesis, Inc.	Cat#: MOG3555-P-5
Adjuvant, Complete H37Ra	BD Difco	Cat#: 231131
M. tuberculosis H37Ra	BD Difco	Cat#: 231141
Pertussis toxin	List Biological Laboratories, Inc.	Cat#: 180
Vancomycin Hydrochloride	Research Products International Corp.	Cat#: V06500
Fluorescein sodium salt	Sigma-Aldrich	Cat#: F6377
Critical commercial assays		
Trypsin Activity Assay Kit (Colorimetric)	Abcam	Cat#: Ab102531
PowerSoil DNA Isolation Kit	Mo Bio Laboratories, Inc.	Cat#: 12888
RNeasy Mini Kit	Qiagen	Cat#: 74106
Fast SYBR Green Master Mix	ThermoFisher Scientific	Cat#: 4385612
HotMaster Taq DNA Polymerase	QuantaBio	Cat#: 2200300
HotMasterMix	QuantaBio	Cat#: 2200400
Deposited data		
16S rRNA gene sequences	This paper	SRA: PRJNA1016427
Experimental models: Organisms/strains		
Mouse: C57BL/6J	The Jackson Laboratory	Stock#: 000664
Mouse: C57BL/6J germ-free	Icahn School of Medicine at Mount Sinai gnotobiotic facility	N/A
Oligonucleotides		
See Table S1		N/A
Software and algorithms		
Trimmomatic v0.39	Bolger, Lohse, & Usadel[67]	https://github.com/usadellab/Trimmomatic
FLASH (Fast Length Adjustment of Short Reads)	Magoč & Salzberg[68]	https://sourceforge.net/projects/flashpage/; RRID: SCR_005531
QIIME 1 (Quantitative Insights Into Microbial Ecology)	Kuczynski et al.[69]	http://qiime.org/index.html; RRID:SCR_008249
PhiX Control v3 Library	Illumina	Cat#: FC-110-3001
BLASTN (Basic Local Alignment Search Tool)	National Center for Biotechnology Information	https://blast.ncbi.nlm.nih.gov/Blast.cgi?PROGRAM=blastn&PAGE_TYPE=BlastSearch&BLAST_SPEC=&LINK_LOC=blasttab&LAST_PAGE=blastn; RRID: SCR_001598
Bowtie2	Langmead and Salzberg[70]	http://bowtie-bio.sourceforge.net/bowtie2/index.shtml; RRID: SCR_016368
RDP (Ribosomal Database Project)	Wang et al.[71]	http://rdp.cme.msu.edu; RRID: SCR_022773

(*Continued on next page*)

Continued

REAGENT or RESOURCE	SOURCE	IDENTIFIER
Resphera Insight (v2.2)	Resphera Biosciences Shaikh et al., 2021[65]	https://respherabio.com/
CUTIE (Correlations Under The InfluencE)	Bu et al.[44]	https://github.com/clemente-lab/CUTIE.git
ImageJ	Schneider et al.[72]	https://imagej.net/ij/index.html; RRID: SCR_003070
Prism v9.3.1	Graphpad Software	https://www.graphpad.com/; RRID: SCR_002798
Other		
Illumina Inc.		https://www.illumina.com/

RESOURCE AVAILABILITY

Lead contact

Information and requests for resources and reagents should be directed to the Lead Contact, Dr. Stephanie K. Tankou (stephanie.tankou@mssm.edu).

Materials availability

This study did not generate new unique reagents.

Data and code availability

16S rRNA sequencing data have been deposited at NCBI Sequence Read Archive (SRA) and are publicly available as of the date of publication. Accession numbers are listed in the key resources table.
This paper does not report original code.
Any additional information required to reanalyze the data reported in this paper is available from the lead contact upon request.

EXPERIMENTAL MODEL AND STUDY PARTICIPANT DETAILS

Animals

C57BL/6J female mice were obtained from the Jackson Laboratory and kept in a specific pathogen-free facility at the Harvard Institute of Medicine or the Icahn School of Medicine at Mount Sinai on a 12-h light/dark cycle. C57BL/6J germ-free female mice were obtained from the Icahn School of Medicine Gnotobiotic Core Facility and kept in a specific pathogen-free facility in the Icahn building at Mount Sinai. Mice were all 8-10 weeks of age and cohoused, 3-5 mice per cage from the same experimental condition per cage. Animals were allowed to acclimate for a total of 5 days before initiation of treatment. Upon arrival at the animal facility, mice are housed in groups of 3-5 per cage by the mice facility staff. Two days after arrival, mice are re-grouped so that each experimental group receives mice from all the cages that were set up on arrival. At this stage, mice have not undergone any experimental manipulations and are indistinguishable from one another. Groups are formed by simply redistributing the mice and exchanging bedding.

Mice were fed an *ad-libitum* diet of PicoLab Rodent Diet 5053 and distilled water at neutral pH provided by the animal facility. Animals were housed in a biosafety level 2 facility using autoclaved cages and aseptic handling procedures. All animal experiments were approved by the International Animal Care and Use Committee (IACUC) at Harvard Medical School or Icahn School of Medicine at Mount Sinai and executed in accordance with the approved animal experiment guidelines.

EAE induction

EAE was induced by immunization 8 to 10-week-old female C57BL/6J mice with 250 μg MOG_{33-55} peptide (Genemed Synthesis) emulsified in complete Freund's adjuvant (CFA) (BD Difco) per mouse, injected subcutaneously into each flank, followed by intraperitoneal injection of 150 ng of pertussis toxin (PT) (List Biological Laboratories, Inc.) per mouse on day 0. A second intraperitoneal injection of 300 ng of PT was administered on day 2. Clinical signs of EAE were assessed according to the following score: 0, no signs of disease; 1, loss of tone in the tail; 2, hind limb paresis; 3, hind limb paralysis; 4, tetraplegia; 5, moribund.

Vancomycin treatment

8–10-week-old C57BL/6J female mice received vancomycin 0.5mg/mL (Research Products International Corp.) in drinking water starting 14 days prior to EAE induction and throughout the duration of the experiment.

METHOD DETAILS

Feces collection, processing, and storage

Feces were collected across several time points spanning pre- and post- immunization states: before vancomycin treatment/EAE induction (day -14), on vancomycin treatment/pre-EAE induction (day 0), and on vancomycin treatment/post-EAE induction (days 3, 7, and 20). Multiple stool pellets from each mouse were collected into a 1.5 ml Eppendorf tube immediately upon defecation. Fecal samples were immediately flash frozen and stored in a -80°C freezer until processed.

Tissue collection

At the end of experiments, mice were intracardially perfused with PBS. Intestinal tissues were cleaned of feces and Peyer's patches removed. To isolate intestinal epithelial cells, terminal ileum samples were incubated in PBS containing EDTA for 30 minutes at 4°C. Next, ileum samples were vortexed vigorously and subsequently filtered through a cell strainer. The filtered medium was spun for 10 minutes at 1400 rpm at 4°C to pellet intestinal epithelial cells. The epithelial cell pellets were then resuspended in buffer RLT (RNeasy kit, Qiagen) for RNA isolation. Terminal ileums were collected in RNA later or RIPA buffer for RNA or protein extraction respectively.

Blood collection

Mice were restrained manually by scruffing the skin of the dorsal neck. A 5-mm lancet (Fisher, Cat# NC9891620) was used to puncture the facial vein on the right side of the face. Blood was allowed to drip freely into a microtainer tube blood collection with lithium heparin (Fisher, Cat#13-680-62). Hemostasis was achieved by using clean, dry gauze applied directly to the access site. Plasma was separated from cellular fraction by centrifugation and subsequently stored in -80°C freezer.

In-vivo permeability assay

In vivo intestinal permeability was performed using Sodium Fluorescein (Sigma, Cat# F6377). Briefly, food was withdrawn for 3h after which, mice were gavaged with 200μL of Sodium Fluorescein (NaF) solution at concentration of 0.1mg/mL. 3 hours post NaF administration, serum was collected after facial vein puncture and fluorescence intensity was measured at 485/528 nm using a microplate reader. NaF concentrations were determined from standard curves generated by serial dilution of NaF. NaF concentrations were normalized by mouse weight.

Trypsin activity assay

Trypsin activity was measured in fecal samples using a commercially available trypsin assay kit (Abcam, Cat# Ab102531). Feces collected and stored as described above were processed following the manufacturer's instructions. One fecal pellet was used per assay. In this assay, trypsin cleaves a substrate to generate *p*-nitroaniline which was detected at OD = 405nm in a kinetic mode every 2-3 minutes for 1-2 hours at 25°C protected from light using Synergy HTX Multi-Mode microplate reader (BioTek). Since the color intensity is proportional to *p*-nitroaniline content, trypsin activity can be accurately measured following the manufacturer's instructions.

Quantitative real-time PCR

Total RNA was isolated from gut tissues using the RNeasy Mini kit (Qiagen) according to the manufacturer's instructions and was stored in -80°C freezer. First strand cDNA synthesis was performed for each RNA sample for up to 1ug of total RNA using a High-Capacity cDNA Reverse Transcription kit (Fisher, Cat# 4374966). Quantitative PCR (qPCR) analysis was conducted using an Applied Biosystems ViiA 7 system (Applied Biosystems). cDNA was amplified using the SYBR Green master mix and specific primers for CCL20, CXCL10, CXCR6, IFN-γ, IL6, IL17A, IL23, PAR2, TNF-α, ZO-1, ZO-2, ZO-3, occludin, claudin-2 and claudin-8 (refer to key resources table for primer sequences). Gapdh and Keratin 8 were used as endogenous control to normalize for differences in the amount of total RNA in each sample for cytokines and tight junctions experiments respectively. PCR was done in duplicate and differential expression was calculated using the delta-CT method.

Immunoblotting

Ileum samples were homogenized in RIPA buffer (Thermofisher, Cat# 89901) and 1X protease inhibitor cocktail (Roche Applied Science). Equal amount of proteins were resolved by polyacrylamide gel electrophoresis. Proteins were transferred to a nitrocellulose membrane and immunoblotting was performed with mouse anti-human PAR2 antibody (Santa Cruz Biotechnology, Cat# SC-13504), and β-actin conjugated to HRP (Abcam, Cat# ab20272) was used as a loading control. For densitometry, nonsaturated developed films were captured with the Bio-Rad ChemiDoc MP imaging system using Image Lab v1 and mean pixel density of each band was measured using ImageJ software (NIH). Data were standardized to actin, and fold change versus control was calculated.

16S rRNA gene sequencing and analysis

Feces were collected as described above. Bacterial DNA was isolated from feces using MoBio PowerLyzer PowerSoil Kit (Qiagen). DNA concentration was quantified using the Quant-iT dsDNA Assay Kit, broad range (Life Technologies) and normalized to 2 ng/μl on a Beckman handling robot. Amplicons spanning variable region 4 (V4) of the bacterial 16S rRNA gene were generated as previously described.[64] Briefly, bacterial 16S rDNA PCR including no template controls were setup in a separate PCR workstation using dual-indexed primers. PCR reactions

contained 1 μM for each primer, 4 ng DNA, and Phusion Flash High-Fidelity PCR Master Mix (Thermo Fisher Scientific). Reactions were held at 98°C for 30 s, proceeding to 50 cycles at 98°C for 10 s, 45°C for 30 s, and 72°C for 30 s and a final extension of 2 min at 72°C. Amplicons were evaluated by gel electrophoresis. The sequencing library was prepared by combining equivolume amounts of each amplicon, size-selected and concentrated using AMPure XP beads (0.8X, Beckman). Library concentration was quantified by Qubit and qPCR, mixed with 15% PhiX, diluted to 4 pM and subjected to paired-end sequencing (Reagent Kit V2, 2x150bp) on an Illumina MiSeq sequencer at the Icahn School of Medicine Microbiome Core Facility.

Paired-end 16S rRNA gene reads were trimmed for quality (target error rate < 0.5%) and length (minimum 200bp) using Trimmomatic, merged using FLASH (Fast Length Adjustment of Short reads), and quality screened using QIIME 1 (Quantitative Insights Into Microbial Ecology). Spurious hits to the PhiX control genome were identified using BLASTN (Basic Local Alignment Search Tool) and removed. Passing sequences were trimmed of primers, evaluated for chimeras and screened for host-associated contaminant using Bowtie2. Chloroplast and mitochondrial contaminants were detected and filtered using the RDP (Ribosomal Database Project) classifier with a confidence threshold of 80%. High-quality 16S rRNA amplicon sequences were assigned to a high-resolution taxonomic lineage using Resphera Insight (v.2.2)[65] for which the performance has been previously benchmarked using high-quality draft genome assemblies of well-defined species from the Human Microbiome Reference Genome Database (http://hmpdacc.org/HMRGD/). Briefly, this method utilizes a manually curated 16S rRNA database of 11,000 unique species, and a hybrid global-local alignment procedure to assign short next-generation sequencing sequences from any region of the 16S rRNA gene to a high-resolution taxonomic lineage. Operational taxonomic units (OTUs) assignment was performed as follows: sequences that could not be confidently assigned to any known species were clustered *de novo*, and clusters were given an OTU number identifier and annotated with a closest relative or set of relatives as previously described.[66] Testing for significant differences in alpha diversity was performed by using a mixed-effects model followed by Sydák's correction for multiple comparisons. Beta diversity was estimated using Bray-Curtis, and distances then used to perform Principal Coordinate Analysis as implemented in QIIME. Differences in beta diversity were tested using PERMANOVA. Taxonomy summary plots were generated based on relative abundances as implemented in QIIME. Compositional differences were determined using linear discriminant analysis effect size (LEfSe) with alpha set at 0.05 and the effect size set at greater than 2. CUTIE correlation analysis, which significantly reduces false positives while increasing sensitivity against false negatives, was used to identify significant correlations between relative abundance of bacterial taxa and fecal trypsin activity and cumulative EAE clinical score.[44]

QUANTIFICATION AND STATISTICAL ANALYSIS

All statistical analyses were performed using GraphPad Prism software (GraphPad Software, San Diego, CA, USA). Statistical tests, sample sizes, and p values are indicated within figure legends.